Optimal Trajectory Generation for a Glider in Time-Varying 2D Ocean Flows B-spline Model

Weizhong Zhang, Tamer Inanc, Sina Ober-Blöbaum, and Jerrold E. Marsden

Abstract— The problem of showing that Lagrangian Coherent Structures (LCS) are useful in determining near optimal trajectories for autonomous underwater vehicles (AUVs) known as gliders is investigated. This paper extends our preliminary results in couple ways. First, the ocean current flows are modeled by 3D B-spline functions in which the input variables are latitude, longitude and time, and the output variable is the ocean current velocity in 2D. The 3D (2D and time-varying) B-spline model of the ocean current is utilized in the Nonlinear Trajectory Generation (NTG) algorithm to find the optimal trajectory of the glider. The trajectories found using the 2D and time-varying B-spline ocean flows model are compared with the trajectories from 2D B-spline model in which the time is assumed to be constant in the ocean current model. In the second part of the paper, the dynamical glider model is established and controlled by gyroscopic forces rather than the simplified kinematic glider model as in the previous work. Finally, numerical solutions of several scenarios and animations of glider trajectories are presented. The results show that the 2D and time-varying B-spline ocean model not only can make the whole trajectory generating process much easier, but also the glider can reach the same destination in a comparable time and with much less energy than it does with the previous 2D ocean current model for both the kinematic and dynamic glider models. Both of the kinematic and dynamic glider optimal trajectories, successfully generated with 2D and time varying ocean current B-spline models, are shown to correspond to LCS.

I. INTRODUCTION

Autonomous underwater vehicles (AUVs) including gliders are becoming more and more popular [1], [2], [3]. For example, the oil and gas industry can use the gliders to make the detailed underwater environment map or search mine-like objects before it decides the next step to exploit the resources. The Autonomous Ocean Sampling Network II project (AOSN-II) [4], [5], [6], [7], [8] aims to advance our ability to observe and predict the ocean by bringing together sophisticated new robotic vehicles (gliders) with advanced ocean models. In this paper, we extend our previous work [6] showing that Lagrangian Coherent Structures (LCS) are useful in determining near optimal trajectories for a class of

Weizhong Zhang is a Ph.D student at the Department of Electrical and Computer Engineering, University of Louisville, Louisville, KY 40292. w0zhan08@gwise.louisville.edu

Tamer Inanc is an Assistant Professor at the Department of Electrical and Computer Engineering, University of Louisville, Louisville, KY 40292. t.inanc@louisville.edu

Sina Ober-Blöbaum is a Professor at the Department of Electrical Engineering and Mathematics, University of Paderborn, D-33095 Paderborn, Germany. sinaob@math.uni-paderborn.de

Jerrold E.Marsden is a Professor at the Department of Control and Dynamical Systems, California Institute of Technology, MC 107-81, Pasadena, CA 91125. marsden@cds.caltech.edu
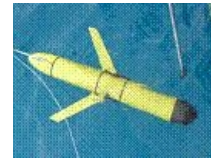
Fig. 1. The SLOCUM glider [9]

gliders. The ocean current flows are modeled by the 3D (2D and time-varying) B-spline functions and the near optimal trajectories of the gliders are obtained using the Nonlinear Trajectory Generation (NTG) method [12]. The results are compared with the trajectories from the 2D ocean flow model in which time is only updated hourly. Furthermore, dynamical glider model is established and controlled by gyroscopic forces so that position and orientation of the glider are obtained in several numerical simulations.

The paper is organized as follows. Next the problem definition is presented. In Section III, the 3D B-spline ocean flows model is established. Then in Section IV the 3D current model is applied in NTG [12] to determine the kinematic glider optimal trajectory. Section V presents the comparison made between the trajectories from 2D current model and those from 3D model. In Section VI, the dynamical glider model is utilized to obtain more realistic trajectories. Finally we compare our results with the corresponding LCS through animations.

II. PROBLEM DEFINITION

The problem considered here is to extend our previously proposed method [6] for quickly determining near optimal glider trajectories between two fixed points in the ocean based on approximate ocean current data. It will be shown that optimal trajectories computed using NTG software corresponds to LCS obtained using the Direct Lyapunov Exponent method [13]. There are two parts are tackled in this paper. One is to improve the previous 2D (assume the 2D ocean current flows stay constant in one hour) analytical ocean flows model [6], which is required in the NTG formulation, to a 3D (2D current and time-varying model) using B-spline functions. The other is to establish a new dynamical model of the glider. Then, these models are used in the NTG to find near optimal trajectories for the glider.
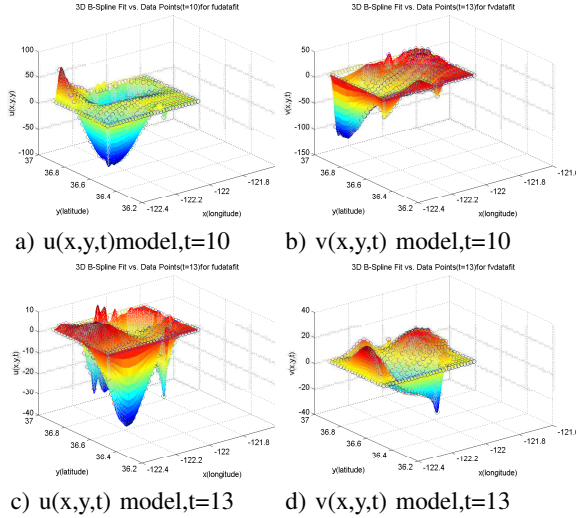
a) u(x,y,t)model,t=10 b) v(x,y,t) model,t=10

c) u(x,y,t) model,t=13 d) v(x,y,t) model,t=13

Fig. 2. The ocean current data and 3D B-spline model at t=10, 13 (hrs)

III. 2D AND TIME-VARYING OCEAN CURRENT FLOWS MODEL

The ocean flows velocity data was obtained hourly from High Frequency Radar stations measuring surface currents around Monterey Bay, CA [14] and processed by Open-Boundary Modal Analysis [15] to smooth the data and fill in the missing data points. In the NTG formulation [6], [12], the cost and the constraints in terms of outputs and their derivatives need to be specified. Therefore, the derivatives of the velocity field with respect to the outputs are required. Numerically computing these derivatives directly from the velocity data sets can easily create convergence problems. Thus, it is best to use approximation techniques to find a smooth analytical model for the data. For this, the B-spline functions are employed, allowing straightforward computation of derivatives.

In this paper ocean current flows model are extended to 3D B-spline functions incorporating the time dependence of the currents explicitly as shown in (1).

$$
\begin{array}{rcl}
u(x,y,t) & = & \sum_{i=1}^{m}\sum_{j=1}^{n}\sum_{k=1}^{o} B_{i,k_{ux}} B_{j,k_{uy}} B_{k,k_{ut}} a_{ijk} \\
v(x,y,y) & = & \sum_{i=1}^{p}\sum_{j=1}^{r}\sum_{k=1}^{s} B_{i,k_{vx}} B_{j,k_{vy}} B_{k,k_{vt}} b_{ijk}
\end{array}
\tag{1}
$$

where a_{ijk} and b_{ijk} represent coefficients of B-spline for $u(x,y,t)$ and $v(x,y,t)$, respectively. $B_{i,k}$, $B_{j,k}$ and $B_{k,k}$ represent B-spline basis functions for the $x-$, $y-$ and $t-$ direction, respectively. The order of the polynomials used were $k_{ux} = k_{uy} = k_{vx} = k_{vy} = k_{ut} = k_{vt} = 4$ and the number of the coefficients were $m = p = 32$, $n = r = 22$ and $o = s = 25$, which are determined by the original data. In order to visualize the models, the time is fixed as it is 2D function. The results in Fig. 2 are similar with the 2D case shown in [6] as expected.

Fig. 3 and Fig. 4 show the 3D B-spline ocean flows models changing with time where x is fixed at -122.3061 (deg) for ease of visualization purposes only.
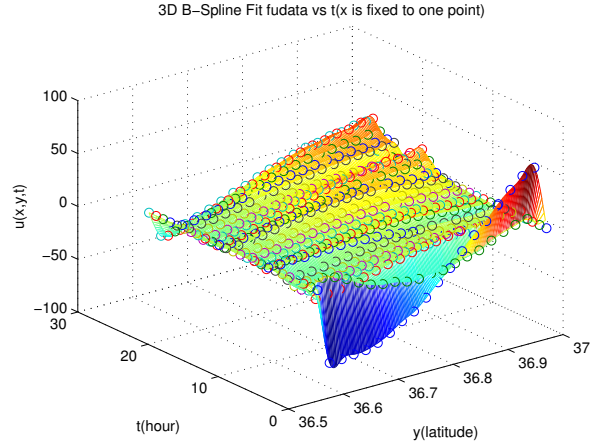

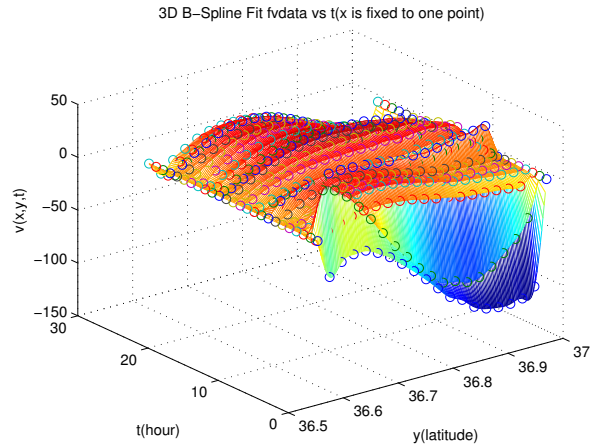Fig. 3. The ocean current data and 3D B-Spline model for u(x,y,t) when x is fixed at (-122.3061)

Fig. 4. The ocean current data and 3D B-Spline model for v(x,y,t) when x is fixed at (-122.3061)

IV. OPTIMAL CONTROL OF KINEMATIC GLIDER

The optimal control problem considered here is to find optimal glider trajectories, -in the case of time, or energy, or time and energy -, between two fixed points in the ocean utilizing recently developed NTG method. The same start and destination points as in [6] are used for comparison.

$$
\begin{array}{rcl}
\mathbf{x}(t_0) & = & (-122.178(\text{deg}), 36.8557(\text{deg})) \\
\mathbf{x}(t_f) & = & (-122.242(\text{deg}), 36.6535(\text{deg}))
\end{array}
\tag{2}
$$

The kinematic glider model as in [6] is considered:

$$
\begin{array}{rcl}
\dot{x} & = & V\cos\theta + u \\
\dot{y} & = & V\sin\theta + v
\end{array}
\tag{3}
$$

where V is the speed of the glider, θ is the orientation of the glider, $u(x,y,t)$ and $v(x,y,t)$ are the components of the ocean currents in the x and y direction, respectively. θ and

V are the control inputs. The pair $(u(x, y, t), v(x, y, t))$ is referred to as the (time-dependent) velocity field.

The Nonlinear Trajectory Generation (NTG) algorithm developed by Milam et al. [12] solves constrained nonlinear optimal control problems in real time. The main advantage of NTG compared to other dynamic optimization methods is that it can quickly provide sub-optimal solutions, which makes it very useful for real-time applications. In addition, linear as well as nonlinear constraints and cost functions can be included in the problem formulation of NTG. The general NTG framework can handle both spatial and temporal constraints.

A. Cost Function

The cost function for this problem is a weighted sum of a temporal cost and an energy cost as follows:

$$
\begin{aligned}
J \quad &= W_t T \\
&+ \int_0^1 W_u \left(\left(\frac{\dot{x}}{T} - u \right)^2 + \left(\frac{\dot{y}}{T} - v \right)^2 \right) T d\tau
\end{aligned} \tag{4}
$$

where $\dot{\mathbf{x}} = \frac{dx}{d\tau}$, $\dot{\mathbf{y}} = \frac{dy}{d\tau}$, W_t and W_u represent the weighting on the total mission time and energy expenditure, respectively. Note that the T terms in the integral, representing the unknown final mission time, and the integral bounds ranging from 0 to 1 are both due to introducing time as a state variable in the NTG formation which is not straight forward. This is explained in details in [6].

B. Constraints

Constraint functions are given as [6]:
- (Linear) Initial Constraints:

$$-122.1780 - \epsilon(\deg) \le x(0) \le -122.1780 + \epsilon(\deg)$$
$$36.8557 - \epsilon(\deg) \le y(0) \le 36.8557 + \epsilon(\deg)$$
$$0 \le T \le 48 \; hours$$

- (Linear) Final Constraints:

$$-122.2420 - \epsilon(\deg) \le x(T) \le -122.2420 + \epsilon(\deg)$$
$$36.6535 - \epsilon(\deg) \le y(T) \le 36.6535 + \epsilon(\deg)$$

- (Nonlinear) Trajectory Constraints:

$$1 \le \left(\frac{\dot{x}}{T} - u \right)^2 + \left(\frac{\dot{y}}{T} - v \right)^2 \le 1600$$

The properties of the trajectories are listed in TABLE. I. In this table, *min E*, *min TE* and *min T* represent minimizing the energy, time and energy and time, respectively. T_f is the final mission time for the glider to travel from the start point to the final point. *Time* represents the actual running time of the NTG algorithm to find the (near) optimal solution. *Energy Cost* is the energy of the glider to travel from start to final point

Fig. 5 shows the trajectories and Fig. 6 shows that the constraints on the glider velocities are satisfied. In these figures, red, blue and green lines correspond to the *min E*, *min TE*, and *min T* trajectories, respectively.

TABLE I
KINEMATIC GLIDER IN 3D B-SPLINE OCEAN CURRENT MODELS

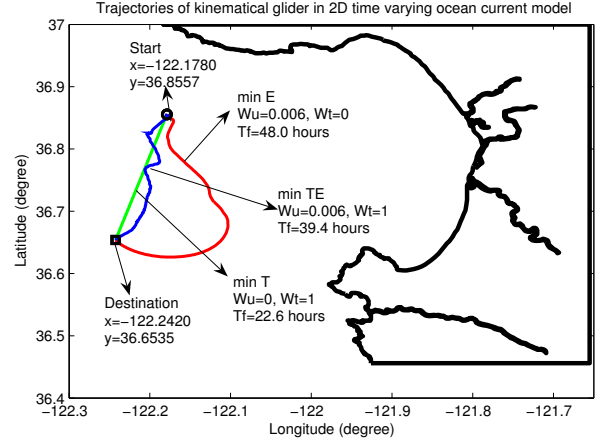| $In3Dmodel$	T_f(hrs)	$Time(s)$	$EnergyCost(cm^2/s)$
$minE$	48.00	2.72	2.7538e4
$minTE$	39.38	1.43	9.0038e4
$minT$	22.60	0.5	1.3209e5

Fig. 5. Trajectories of kinematical glider in 3D ocean current model

V. COMPARISON OF KINEMATIC GLIDER TRAJECTORIES IN 2D AND 3D B-SPLINE OCEAN CURRENT MODELS

In the following the trajectories of the kinematic glider found using 2D and 3D (2D plus time-varying) B-spline ocean models are compared. These two types of ocean current flows models are applied into NTG with the same kinematic glider model, refer to (3), cost and constraint functions.

The optimal trajectories minimizing the energy by using the two models are shown in Fig. 7. The dotted line shows the concatenated trajectories found using 2D B-spline ocean model by running the NTG algorithm several times, once for every hour. The solid blue line shows the glider trajectory found using the 3D B-spline ocean model. The properties from the two models are listed in TABLE. II.

Fig. 7 indicates that the minimizing-energy trajectories from 3D and 2D ocean current models are almost the same. Hence, it shows that the assumption in [6] that the velocity fields are constant over hourly intervals is reasonable in this case. However, the minimizing-time-and-energy trajectories obtained from 3D and 2D ocean models look different clearly shown in Fig. 8. The reason is that for minimizing time-and-

TABLE II
KINEMATIC GLIDER IN 3D VERSUS 2D B-SPLINE OCEAN CURRENT
MODELS

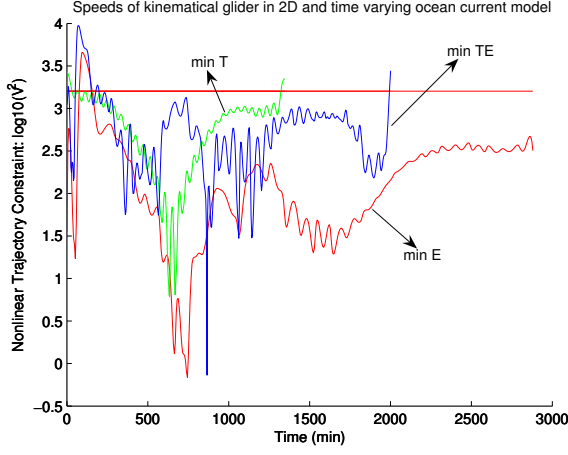| $3D/2D$	$T_f(hrs)$	$Time(s)$	$EnergyCost(cm^2/s)$
$minE$	48.00/45.84	2.72/64.42	2.7538e4/4.039e5
$minTE$	39.38/39.31	1.43/42.77	9.0038e4/4.178e5

Fig. 6.   Kinematical glider speed in the new ocean current model
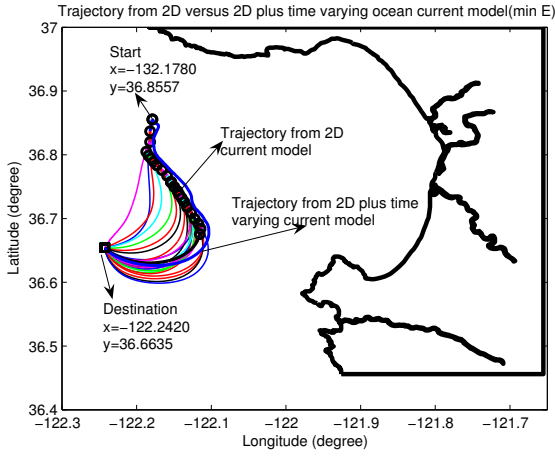

Fig. 7.   Kinematic glider min E trajectories in two models
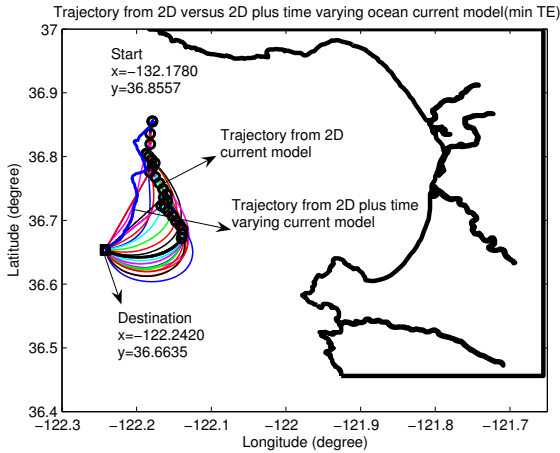

Fig. 8.   Kinematic glider min TE trajectories in two models

energy when the start point and velocity field are different, the glider might decide to choose a different way based on the current flows and the position. It will not necessarily move with the direction of the ocean flow as in the *min E* case. Even though the trajectories are different in the case of minimizing energy and time, the shapes and curves of these two trajectories are still similar with each other.

VI. OPTIMAL CONTROL OF DYNAMIC GLIDER

In this section, the dynamics of the glider is taken into account. The glider is assumed to be actuated by gyroscopic forces F_{gyr}, which implies that the relative forward speed of the glider is constant. And the orientation of the glider cannot change instantly and the control force is the change in the orientation of the glider. The dynamic model of the glider is listed in the following:

$$
\begin{aligned}
\ddot{\mathbf{x}} &= -V\frac{d\theta}{dt}\sin\theta + \dot{u} \\
\ddot{\mathbf{y}} &= V\frac{d\theta}{dt}\cos\theta + \dot{v}
\end{aligned}
\tag{5}
$$

According to (3), then the dynamical glider model can be expressed as:

$$
\begin{aligned}
\ddot{\mathbf{x}} &= -\frac{d\theta}{dt}(\dot{y}-v) + \dot{u} \\
\ddot{\mathbf{y}} &= \frac{d\theta}{dt}(\dot{x}-u) + \dot{v}
\end{aligned}
\tag{6}
$$

The gyroscopic force is given by:

$$
F_{gyr} = \begin{pmatrix} -\dfrac{d\theta}{dt}(\dot{y}-v) \\ \dfrac{d\theta}{dt}(\dot{x}-u) \end{pmatrix}
\tag{7}
$$

The gyroscopic force acts proportional to the relative velocity between fluid and the glider.

A. Cost Function

For the dynamic glider model, the control force is the F_{gyr}. Therefore, the cost function is shown in the following:

$$
J = W_t T + W_u \int_0^T \| F_{gyr} \|^2 dt
$$

The cost function can be further expressed utilizing (5) and (7) as:

$$
J = W_t T + W_u \int_0^T \left((\ddot{x}-\dot{u})^2 + (\ddot{y}-\dot{v})^2 \right) dt
$$

When $\tau = \frac{t}{T}$, we obtain the cost function for the dynamic glider after introducing the time as a state variable in the NTG formulation [6] as:

$$
J = W_t T + W_u \int_0^1 \left(\left(\frac{\ddot{x}}{T^2} - \dot{u} \right)^2 + \left(\frac{\ddot{y}}{T^2} - \dot{v} \right)^2 \right) T d\tau
$$

B. Constraints

The constraints for the dynamic glider model are almost the same as the ones in the kinematical glider model. One more constraint related with the control force F_{gyr} is added since it cannot be infinitely large. Therefore, the constraints for the glider orientation change are arbitrarily introduced as shown in (8):

$$-18 \left(\deg/s \right) \leq \frac{d\theta}{dt} \leq 18 \left(\deg/s \right) \tag{8}$$

The constraint function (8) can be further expressed utilizing (3) and (6), as:

$$-18 \left(\deg/s \right) \leq \frac{\ddot{y} - \dot{v}}{\dot{x} - u} \leq 18 \left(\deg/s \right) \tag{9}$$

where

$$\dot{x} = dx/dt, \ddot{y} = d^2 y/dt^2 \tag{10}$$

After applying the dynamic glider model (6) and 3D B-spline ocean current models (1) in NTG, the trajectories of the dynamic glider are plotted in Fig. 9. Fig. 10 shows the speed constraints of the glider. The properties of the trajectories from the dynamic glider model
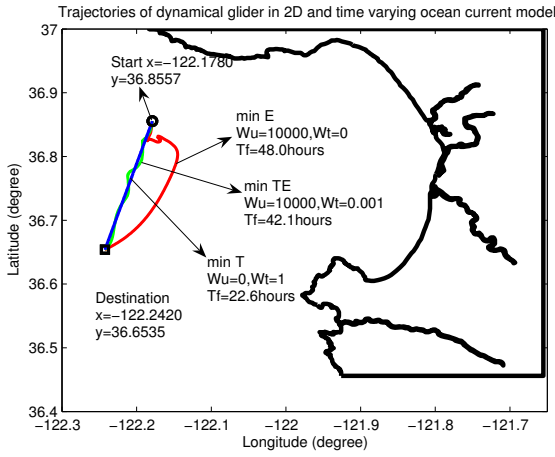

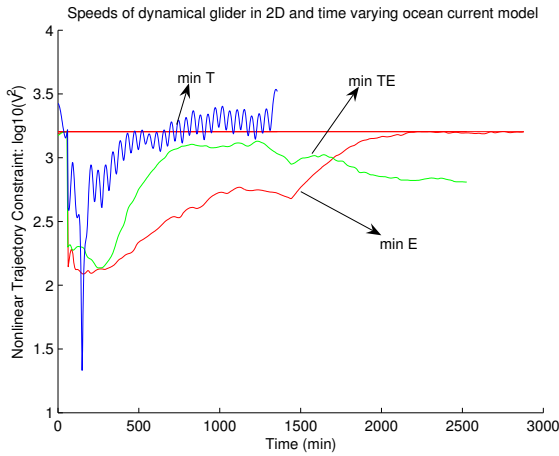Fig. 9.   Trajectories of kinematical glider in 3D ocean current model

Fig. 10.   Dynamical glider speed in the new ocean current model

are listed in the following TABLE. III, *3D (Dyn)* represents the trajectories obtained from the 3D B-Spline ocean current models and from the dynamic glider model. *Tf*, *Time* and *Energe Cost* represents the same as in TABLE. I.

$3D(Dyn)$	T_f(hrs)	$Time(s)$	$EnergyCost(cm^2/s)$
$minE$	48.00	17.87	5.642E3
$minTE$	42.12	17.60	6.9491E3
$minT$	22.60	0.95	1.1389E4

The orientation of the glider, shown in Fig. 11, is obtained by using (11).

$$\tan\theta = \frac{\dot{y} - v}{\dot{x} - u} \tag{11}$$

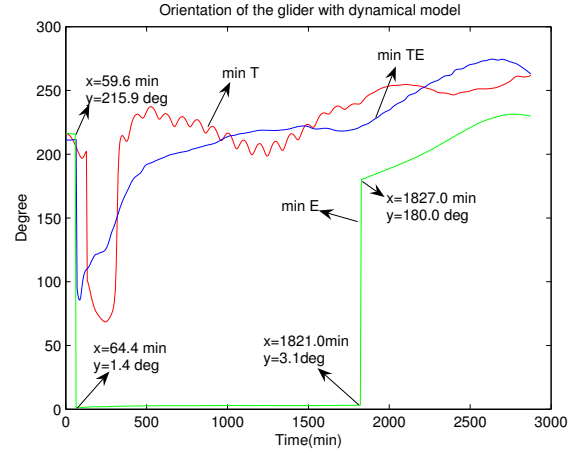The figure of the orientation:

Fig. 11.   Orientation of the dynamica glider in 3D ocean current model

The two sharp orientation changes shown in Fig. 11 do not violate the constraint given in (8). Specifically, the sharp orientation turn one on the left of green trajectory is

$$\begin{aligned}
\frac{d\theta}{dt} &= (1.4 - 215.9)/(64.4 - 59.6)/60 \\
&= -0.7 deg/s \geq -18 deg/s
\end{aligned} \tag{12}$$

The sharp turn on the right of the green trajectory is

$$\begin{aligned}
\frac{d\theta}{dt} &= (180.0 - 3.1)/(1827.0 - 1821.0)/60 \\
&= -0.5 deg/s \leq 18 deg/s
\end{aligned} \tag{13}$$

Therefore, the trajectory is satisfied with the constraints about the glider orientation change.

VII. ANIMATION OF GLIDER AND OCEAN CURRENT

The animation of the glider and ocean current is obtained and the results are shown in Fig. 12 and Fig. 13 for the kinematic and dynamic glider models, respectively. *These new results strengthen our previous hypothesis [6] that LCS in the ocean reveal efficient or near-optimal routes for glider transport*. In Fig. 12 and Fig. 13, we have superimposed instances of the min E trajectories given in Fig. 7 and Fig. 9 with the corresponding LCS fields at that time, respectively. These figures should be thought of as snapshots of a

movie which shows the progression of the LCS and the progression of the glider path together. One can see that there is indeed a good correspondence between the optimal trajectory and the LCS.
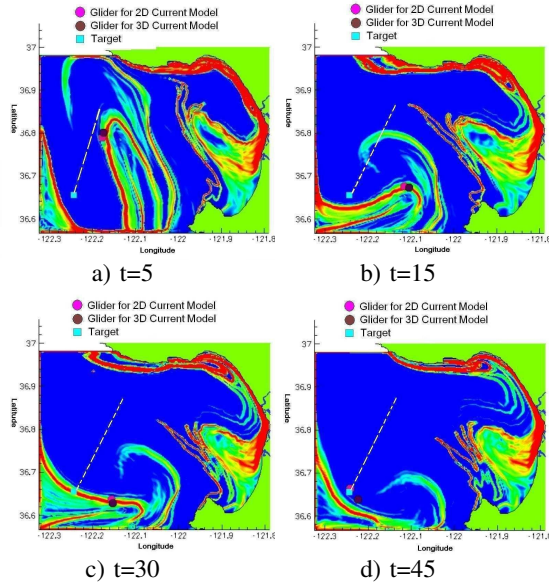

Fig. 12. The figure shows the correspondence with the optimal trajectories shown in Fig. 7 and an LCS. Note that the red and pink in the figures near the LCS represents the location of the AUVs while the blue represents the final target location.
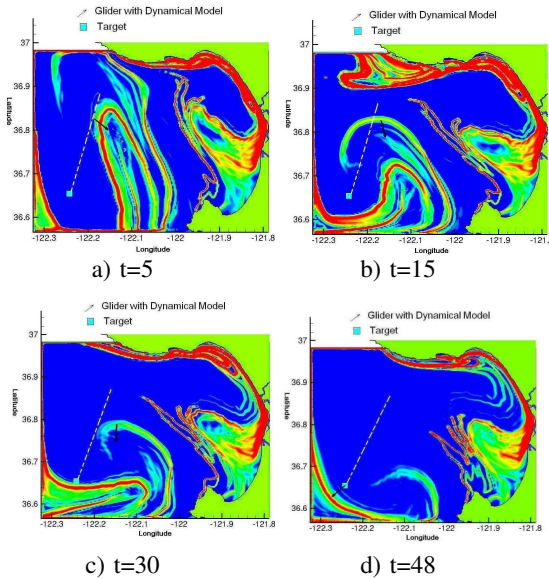

Fig. 13. The figure shows the correspondence with the optimal trajectories shown in Fig. 9 and an LCS. Note that the red and pink in the figures near the LCS represents the location of the AUVs while the blue represents the final target location.

VIII. CONCLUSION

In this paper, we have strengthened our previous hypothesis [6] that LCS in the ocean reveal efficient or near-optimal routes for glider transport. As an extension to our previous work [6], the ocean current flows 3D (2D and time-varying) B-spline models are established incorporating the time explicitly. These models are applied in the NTG to find the optimal glider trajectories and the results are compared with the previous 2D B-spline models. The results show that the 3D ocean current model has produced similar trajectories with less energy cost. Next, the dynamics of the glider is considered in the glider model. The gyroscopic force is applied to control the glider orientation. The results enhance our previous hypothesis showing that the trajectory of minimizing energy is reasonably consistent with the LCS.

IX. ACKNOWLEDGMENTS

REFERENCES

[1] R. Bachmayer, N. E. Leonard, J. Graver, E. Fiorelli, P. Bhatta, D. Paley, "Underwater Gliders: Recent Developments and Future Applications", p195, 2004 *International Symposium on Underwater Technology*, Apr 20-23, Taipei, Taiwan, China.

[2] D. L. Rudnick, R. E. Davis, C. C. Eriksen, D. M. Fratantoni, and M. J. Perry, "Underwater gliders for ocean research", *Marine Technology Society Journal*, Vol. 38, Number 1, Spring 2004.

[3] S. A. Jenkins, D. E. Humphreys, Jeff Sherman, Jim Osse, Clayton Jones, Naomi Leonard, Joshua Graver, Ralf Bachmayer, Ted Clem, Paul Carroll, Philip Davis, Jon Berry, Paul Worley, and Joseph Wasyl, underwater Glider System Study. May 6, 2003. Scripps Institution of Oceanography Technical Report. Available: http://repositories.cdlib.org/sio/techreport/53/

[4] Autonomous Ocean Sampling Network Homepage, Edited Aug.9, 2006. Available: *http://www.mbari.org/aosn/default.htm*

[5] B. Curtin, J. G. Bellingham, J. Catipovic, and D. Webb, "Autonomous Oceanographic Sampling Networks",*Oceanography*, 6:86-94, 1989.

[6] Tamer Inanc, Shawn C. Shadden and Jerrold E. Marsden, "Optimal Trajectory Generation in Ocean Flows". p674, *2005 American Control Conference*, June 8-10, 2005, Portand, OR.

[7] Fumin Zhang, David M. Fratantoni, Derek Paley, John Lund and Naomi Ehrich Leonard, "Control of Coordinated Patterns for Ocean Sampling", *International Journal of Control*, special issue on Navigation, Guidance and Control of Uninhabited Underwater Vehicles, Vol. 80, No. 7, July 2007, pp. 1186-1199.

[8] Pradeep Bhatta, Edward Fiorelli, Francois Lekien, Naomi Ehrich Leonard. et al, "Coordination of an Underwater Glider Fleet for Adaptive Ocean Sampling", *in Proc. International Workshop on Underwater Robotics, Int. Advanced Robotics Programmed (IARP)*, Genoa, Italy, November 2005.

[9] Stommel,H.1989."The Slocum Mission", *Oceanography*, 2(1), 22-25.

[10] Joshua G. Graver, Ralf Bachmayer, Naomi Ehrich Leonard and David M. Fratantoni, "Underwater Glider Model Parameter Identification", *in Proc. 13th Int. Symp. on Unmanned Untethered Submersible Technology (UUST)*,Durham, NH, Aug.2003.

[11] Sherman, R. E. Davis, W. B. Owens, and J. Valdes. "The autonomous underwater glider spray", *IEEE J.Oceanic Engin.*, 26(4), 437-446.

[12] M. B. Milam, K Mushambi, and R. M. Murray, "New Computational Approach to Real-Time Trajectory Generation for Constrained Mechanical Systems", *in Conference on Decision and Control*, 2000.

[13] G. Haller, "Lagrangian Coherent Structures from Approximate Velocity Data", *Physics of Fluids*, Vol 14, No 6,1851-1861, 2002.

[14] J. D. Paduan and L. K. Rosenfeld, "Remotely Sensed Surface Currents in Monterey Bay from Shore-Based HF Radar (CODAR)", *J.Geophys. Res.*, 101, 20669-20686.

[15] F. Lekien, C. Coulliette, R. Bank, J. Marsden, "Open-Boundary Modal Analysis: Interolation, Extrapolation and Filtering",*Journal of Geophysical Research Oceans*, Vol. 109, 2004.